Chemical Science

ROYAL SOCIETY OF CHEMISTRY

EDGE ARTICLE

View Article Online
View Journal | View Issue

Cite this: *Chem. Sci.*, 2024, **15**, 13523

All publication charges for this article have been paid for by the Royal Society of Chemistry

Combining photocontrolled-cationic and anionic-group-transfer polymerizations using a universal mediator: enabling access to two- and three-mechanism block copolymers†

Brandon M. Hosford, ‡ William Ramos ‡ and Jessica R. Lamb *

An ongoing challenge in polymer chemistry is accessing diverse block copolymers from multiple polymerization mechanisms and monomer classes. One strategy to accomplish this goal without intermediate compatibilization steps is the use of universal mediators. Thiocarbonyl thio (TCT) functional groups are well-known mediators to combine radical with either cationic or anionic polymerization, but a sequential cationic-anionic universal mediator system has never been reported. Herein, we report a TCT universal mediator that can sequentially perform photocontrolled cationic polymerization and thioacyl anionic group transfer polymerization to access poly(ethyl vinyl ether)-*block*-poly(thiirane) polymers for the first time. Thermal analyses of these block copolymers provide evidence of microphase separation. The success of this system, along with the established compatibility of radical polymerization, enabled us to further chain extend the cationic-anionic diblock using radical polymerization of *N*-isopropylacrylamide. The resulting terpolymer represents the first example of a triblock made from three different monomer classes incorporated *via* three different mechanisms without any end-group modification steps. The development of this simple, sequential synthesis using a universal mediator approach opens up new possibilities by providing facile access to diverse block copolymers of vinyl ethers, thiiranes, and acrylamides.

Received 16th April 2024
Accepted 19th July 2024

DOI: 10.1039/d4sc02511c

rsc.li/chemical-science

Introduction

Block copolymers (BCPs) are important and versatile materials due to their unique properties and functions, which are dictated by their composition and microstructure.[1–3] Most BCPs are made from a single polymerization mechanism where compatible monomers are added sequentially.[4–6] However, this approach limits the accessible chemical space to similar monomer classes[7–11] or to a prescribed addition order to maintain the active chain-end.[6,12–16] Ideally, polymer chemists would not be confined to this paradigm, such that disparate monomers could be combined to access an expanded property space. To accomplish this goal, it is necessary to develop new ways to easily incorporate different polymerization mechanisms (*e.g.*, cationic, anionic, and radical) into a single material. Combining cationic and anionic mechanisms has been particularly understudied,[17] presumably due to the incompatibility of their reactive intermediates.

Common methods to combine multiple mechanisms – such as homopolymer coupling,[18–20] end-group modification,[21–34] or the use of multi-functional initiators[35–38] – require additional

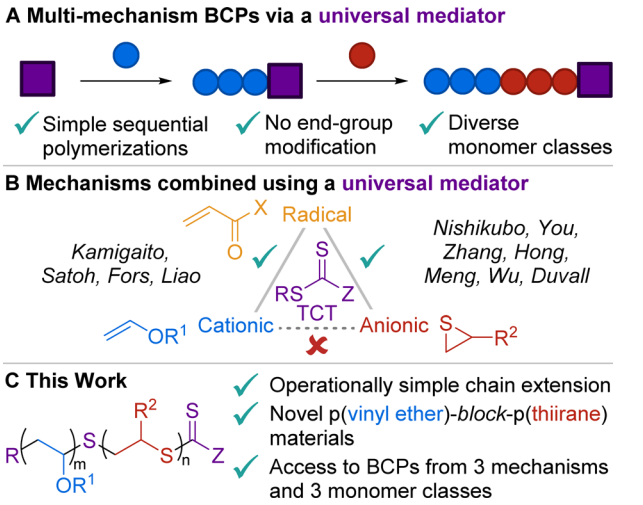

Fig. 1 (A) General scheme for the synthesis of BCPs using a universal mediator. (B) Previous TCT universal mediator reports for radical/cationic and radical/anionic polymerizations. (C) This work combining cationic and anionic polymerizations using a TCT universal mediator.

Department of Chemistry, University of Minnesota—Twin Cities, 207 Pleasant Street SE, Minneapolis, MN 55455, USA. E-mail: jrlamb@umn.edu

† Electronic supplementary information (ESI) available. See DOI: https://doi.org/10.1039/d4sc02511c

‡ B. M. H. and W. R. contributed equally to this work.

synthetic steps and/or are limited in the number and arrangement of blocks in the final material. Universal mediators – which are functional groups that can facilitate distinct mechanisms under different conditions – are an elegant solution to these challenges (Fig. 1A). Due to the fact that the mediator stays at the chain end, multi-mechanism BCPs can be made *via* simple sequential polymerizations, and the user is theoretically not limited in the number of blocks accessible. Thiocarbonyl thio (**TCT**) moieties are well-studied universal mediators to sequentially combine radical polymerization with either cationic[39–44] or anionic group transfer[45–50] polymerization, but they have never been reported to mediate cationic and anionic polymerizations (Fig. 1B), possibly due to the opposing natures of these two mechanisms resulting in vastly different reaction condition requirements. Bridging this gap would open new and exciting possibilities to access novel poly(vinyl ether)-*b*-poly(thiirane) materials and to change between all three (*i.e.*, cationic, anionic, and radical) polymerizations without extra compatibilization steps – vastly expanding the available chemical space accessible *via* this streamlined synthetic method. On the basis of the rich literature of cationic[40,51–58] and anionic[45,59,60] homopolymerizations using **TCT**s, we hypothesized that proper selection of the monomers, R and Z groups of the **TCT**,[61,62] and reaction conditions would successfully enable sequential cationic-anionic polymerizations using a universal mediator for the first time.

Herein, we report a straightforward, multi-pot, sequential method that combines photocontrolled cationic polymerization (photo-CP) and thioacyl anionic group transfer polymerization (TAGT) to generate novel BCPs of poly(vinyl ether)s and poly(thiirane)s (Fig. 1C). We identified a viable **TCT** universal mediator and explored [monomer]:[**TCT**] achieving number-average molar mass (M_n) up to 53 kDa and monomer scope of the homopolymerizations. Next, poly(ethyl vinyl ether) (p(EVE)) was chain extended with a variety of thiiranes to form diblock copolymers which were characterized by NMR spectroscopy, size-exclusion chromatography (SEC), thermogravimetric analysis (TGA), and differential scanning calorimetry (DSC). For each BCP, we observed two glass transition temperatures (T_gs), which suggest microphase separation between the blocks.[63] Capitalizing on the success of this method completing the trio of mechanisms using this universal mediator, we further chain extended the BCPs with *N*-isopropylacrylamide (NIPAM) *via* photocontrolled radical polymerization. This novel triblock terpolymer is produced from three different mechanisms and three monomer classes without any end-group manipulations using this universal mediator approach.

Results and discussion

Universal mediator identification

We began our compatibilization efforts by adapting reported reaction conditions for photo-CP[64] and TAGT.[46] For the photo-CP of ethyl vinyl ether (EVE), we used the classic oxidizing photocatalyst 2,4,6-tri-(*p*-methoxyphenyl)pyrylium tetrafluoroborate (**PC**) in dichloromethane (DCM). For TAGT of 3-phenoxypropylene sulfide (POPS), we used tetraphenyl phosphonium chloride (TPPCl) as the nucleophilic catalyst in *N*,*N*-dimethylacetamide (DMAc).

We explored a number of **TCT** mediators, varying the R and Z groups (Table 1) to determine the optimal mediator for both photo-CP and TAGT. We hypothesized that a thioacetal R group would be vital for controlled initiation of photo-CP[44,65,66] because the thioacetal helps facilitate the C–S bond cleavage to

Table 1 Identification of an appropriate universal mediator and optimization for photo-CP of EVE and TAGT of POPS

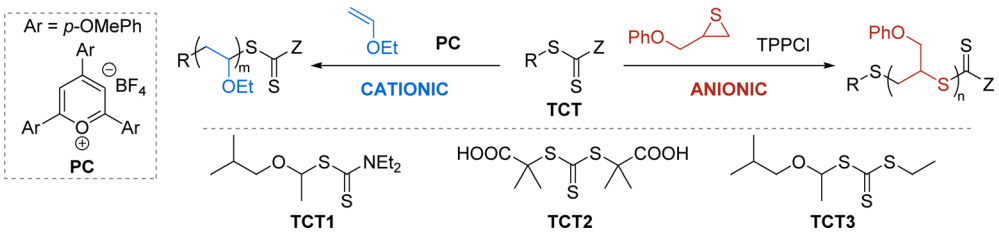

		Cationic (photo-CP)[a]					Anionic (TAGT)[b]			
TCT	Entry	Conv.[c] (%)	$M_{n,theo}$ (kDa)	M_n[d] (kDa)	$Đ$[d]	Entry	Conv.[d] (%)	$M_{n,theo}$ (kDa)	M_n[d] (kDa)	$Đ$[d]
TCT1	1a	95	3.7	3.8	1.13	1b	92	15.8	97.2	3.55
TCT2	2a	>99	3.9	6.2	2.51	2b	>99	17.4	16.5	1.22
TCT3	3a	>99	3.8	3.8	1.34	3b	88	15.6	19.5	1.35
TCT3	4a[e]	<1	—	—	—	4b	n.d.	n.d.	n.d.	n.d.
—	5a	99	—	10.1	1.95	5b	73	—	289.6	1.87
TCT3	6a[f]	98	3.8	4.5	1.17	6b[f]	60	9.92	14.1	1.67

[a] Photo-CP standard conditions: **TCT** (20 μmol, 1 eq.), EVE (50 eq.), **PC** (2.0 mol% relative to **TCT**), DCM (92 mM), RT, 456 nm LED, 6 h. [b] TAGT standard conditions: **TCT** (15 μmol, 1 eq.), POPS (100 eq.), TPPCl (0.33 eq.), DMAc (1.0 mL), 60 °C, 6 h. [c] Determined *via* ^{1}H NMR spectroscopy. [d] Determined *via* SEC in DMF with 0.025 M LiBr against PMMA standards. [e] Polymerization run with no **PC**. [f] Polymerization run with 1.0 mol% of **PC** relative to **TCT**. n.d. = not determined.

generate the cationic chain end. On the other hand, the Z group will dictate the nucleophilic attack of the activated thiolate monomer in TAGT by controlling the electrophilicity of the thiocarbonyl carbon. If the **TCT** is not electrophilic enough, the thiolate can instead directly attack another thiirane monomer, leading to uncontrolled polymerization characterized by a large dispersity and an M_n much larger than the theoretical M_n. As expected, polymerizations with **TCT1**[67] and **TCT2**, which are common **TCT**s used for photo-CP[64] and TAGT,[46,48] respectively, resulted in well-controlled polymerizations for their reported mechanisms (Table 1, entries 1a and 2b), but had poor control for the other polymerization (entries 1b and 2a). The dithiocarbamate of **TCT1** is not electrophilic enough, resulting in uncontrolled TAGT, and **TCT2** lacks the thioacetal R group for efficient photo-CP initiation. Combining the two important features into **TCT3** – a more electrophilic trithiocarbonate with a thioacetal R group – resulted in moderate control for both photo-CP and TAGT (entries 3a and 3b).

Control experiments showed that no p(EVE) was made in the absence of **PC** (entry 4a) and that **TCT** is necessary for controlled polymerization in both cases (entries 5a and 5b). Successful polymerization of EVE without the presence of a mediator is evidence of direct oxidation of the vinyl ether monomer by **PC**, but previous studies have shown that **TCT** oxidation occurs much faster than direct monomer oxidation at low [vinyl ether] : [**TCT**] ratios.[66]

Factors affecting sequential polymerization

During the initial polymerizations, we discovered that p(EVE) is difficult to purify because it is highly soluble (>10 mg mL^{-1}) in a wide range of solvents – hexanes, diethyl ether, tetrahydrofuran, DCM, methanol, and DMAc (see ESI, Section S1.A†). Therefore, it was necessary to explore the effect of the photo-CP components on TAGT. Even a small amount of DCM inhibits TAGT, but both residual monomer and DCM can be completely removed from the polymer by drying in a vacuum oven at 70 °C for 16 hours. Conversely, the **PC** is not volatile, which makes it more challenging to remove. Unfortunately, dialysis was unsuccessful, and precipitation into water resulted in co-precipitation of p(EVE) and **PC**; therefore, we were unable to effectively remove the **PC** from the polymer. Thus, we tested the effect of varying amounts of **PC** on the TAGT (see ESI, Section S2.A†). At high loadings, **PC** inhibits the anionic polymerization (13% conversion in 6 h at 4 mol% **PC** relative to **TCT**). However, at 1 mol% **PC**, most of the activity is retained (60% conversion in 6 h; Table 1, entry 6b). During this exploration, we discovered the photo-CP still achieved 98% conversion at half of our standard loading (entry 6a). Therefore, in order to minimize the amount of **PC** contamination for chain extensions, we continued using the halved **PC** loading moving forward.

Homopolymerization scope

Next, we explored the scope and limitations of **TCT3** as a mediator for both polymerizations. To determine control over a wide molar mass range, we performed a [monomer] : [**TCT3**] screen for photo-CP of EVE and TAGT of POPS (Fig. 2; for tabulated data, see Section S2.B†). Photo-CP performed well when [EVE] : [**TCT**] was 50 : 1 and 100 : 1 – resulting in a close match of M_n to $M_{n,theo}$ and a low dispersity. However, at larger [EVE] : [**TCT**] (200–300 : 1), M_n deviates from $M_{n,theo}$, which is common for photo-CP due to the increased levels of direct monomer oxidation.[66] This oxidation acts as a competing initiation pathway, leading to more chains and resulting in a lower M_n.[68] TAGT performed well for all [POPS] : [**TCT**] screened and resulted in good agreement between M_n and $M_{n,theo}$, achieving molar masses up to 53 kDa while maintaining a low-to-moderate dispersity (<1.55).

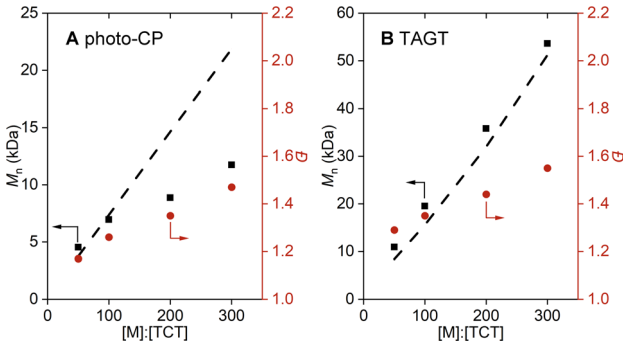

Fig. 2 [Monomer] : [**TCT3**] screen of (A) photo-CP and (B) TAGT homopolymerizations. Black squares: M_n. Red circles: $Đ$. Black dashed line: $M_{n,theo}$. Photo-CP conditions: **TCT** (20 μmol, 1 eq.), vinyl ether, **PC** (0.02 mol% relative to EVE), DCM (92 mM), RT, 456 nm LED, 6 h. TAGT conditions: **TCT3** (4 μmol, 1 eq.), thiirane, TPPCl (0.33 eq.), DMAc (0.27 mL), 60 °C, 6 h.

While **TCT3** has previously been reported for photo-CP of EVE, isobutyl vinyl ether (IBVE), and ^{n}butyl vinyl ether (BVE);[64,66] we attempted to expand the scope to high T_g poly(vinyl ethers)[69,70] from cyclohexyl vinyl ether (CHVE) and 2,3-dihydrofuran (DHF) (Fig. 3A). These monomers achieved full conversion in 6 hours, but SEC analysis showed bimodal distributions for both polymers (Fig. S4 and S5†), which we hypothesize is due to both photocatalytic activation and direct monomer activation. Unfortunately, all poly(vinyl ethers)

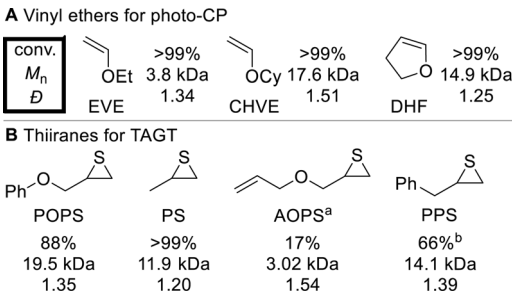

Fig. 3 (A) Vinyl ether and (B) thiirane monomer scope. M_n and $Đ$ determined *via* SEC in DMF with 0.025 M LiBr against PMMA standards. Photo-CP standard conditions: **TCT** (20 μmol, 1 eq.), vinyl ether (50 eq.), **PC** (2.0 mol% relative to **TCT**), DCM (92 mM), RT, 456 nm LED, 6 h. TAGT standard conditions: **TCT3** (4 μmol, 1 eq.), thiirane (100 eq.), TPPCl (0.33 eq.), DMAc (0.27 mL), 60 °C, 6 h. [a]Reaction run for 24 h. [b]Estimated conversion due to overlapping peaks.

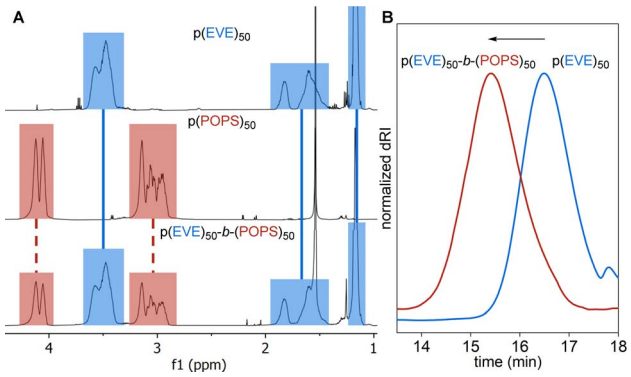

Fig. 4 (A) Stacked ^{1}H NMR spectra of respective homopolymers and p(EVE)$_{50}$-*b*-p(POPS)$_{50}$. (B) Representative SEC traces showing chain extension from p(EVE)$_{50}$ to p(EVE)$_{50}$-*b*-p(POPS)$_{50}$.

beyond p(EVE) were found to be insoluble in DMAc, and thus were not carried onto chain extension trials or pursued further.

Unlike for photo-CP, **TCT3** has never been reported for TAGT. Therefore, we tested common thiirane monomers[46,48,49,59,60] POPS (*vide supra*), propylene sulfide (PS), and allyloxy propylene sulfide (AOPS) in addition to a new monomer, phenyl propylene sulfide (PPS), using this mediator (Fig. 3B). **TCT3** was very effective for PS, reaching >99% conversion to form p(PS) ($M_n = 11.9$ kDa) with a narrow $Đ$ (1.20). AOPS only achieved 17% conversion in 24 hours, resulting in a low molar mass (3.02 kDa), and a slightly elevated $Đ$ (1.54). PPS proceeded with moderate conversion (66%), forming p(PPS) ($M_n = 14.1$ kDa) with a narrow $Đ$ (1.39). Despite the variability in reactivity between the thiiranes, all were tested in the chain extensions with p(EVE). These results showing successful photo-CP and TAGT validate **TCT3**'s promise as a universal mediator for these mechanisms.

Chain-extension of p(EVE)

Following photo-CP, the p(EVE) samples were used as macromediators for chain extension *via* TAGT. Initially, we utilized 50, 100, 200, and 300 monomer equivalents for both EVE and POPS to target p(EVE)-*b*-p(POPS) with a range of block lengths (see Section S2.E†). Excitingly, the ^{1}H NMR spectra show the presence of both blocks (Fig. 4A) and the SEC peaks shift to higher molar masses, indicating the successful chain extension in every case (Fig. 4B and S9–S12†). Due to the challenge of accurately determining degrees of polymerization for BCPs, all polymers were named on the basis of monomer feed (*e.g.*, p(EVE)$_{50}$-*b*-p(POPS)$_{50}$). For BCPs made from p(EVE)$_{200}$ or p(EVE)$_{300}$, bimodal peaks were observed in the SEC. We hypothesize this bimodality arises from the increased amount of direct monomer oxidation, which yields some p(EVE) chains that cannot be extended due to the lack of a **TCT** end group. Despite some loss of control at high molar masses, these chain extensions represent the first examples of sequential cationic-anionic polymerizations using a **TCT** universal mediator.

Unfortunately, during the purification process *via* precipitation in methanol, we encountered fractionation of p(EVE)-*b*-p(POPS) on the basis of the relative composition of the different blocks (Section S2.F†). To avoid this fractionation from interfering with the polymer characterization, the chain extension screen was repeated – focusing on the block lengths that retained control (*i.e.*, 50 and 100 monomer equivalents) – and the resulting BCPs were purified using preparative SEC (prepSEC) (Table 2). As the ratio of [POPS] : [p(EVE)] went up from 50 to 100, the TAGT conversion also went up (compare entries 1 and 2 or 3 and 4), which we hypothesize is due to the higher concentration of thiirane monomer resulting in a chemical environment more similar to a POPS homopolymerization. Additionally, we observe lower conversion of POPS when using p(EVE)$_{100}$ (entries 3–4), possibly arising from more residual **PC** and/or mass transport limitations. Similar to our initial chain extension screen, all BCPs showed clean peak shifts to lower retention times in the SEC relative to p(EVE) homopolymer (see Section S2.G†).

The expanded thiirane scope also cleanly extended p(EVE)$_{50}$ under the standard TAGT conditions (Table 3 and Fig. S21–S23†). The polymerization of PS proceeded rapidly, reaching high conversion (94%) within 3 hours and maintaining a moderate $Đ$ (1.45) (entry 1). On the basis of the lower reactivity of AOPS and

Table 2 Select chain extensions of p(EVE) with TAGT of POPS[a]

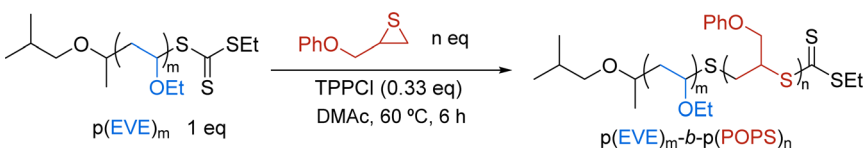

Entry	Starting polymer	[POPS] : [p(EVE)]	Conv.[b] (%)	M_n[c] (kDa)	M_w[c] (kDa)	$Đ$[c]	T_o[d] (°C)	T_g[e] (°C)
1	p(EVE)$_{50}$	50 : 1	55%	10.3	14.7	1.43	283, 376	−30, 18
2	p(EVE)$_{50}$	100 : 1	61%	18.7	27.4	1.47	272, 375	−32, 19
3	p(EVE)$_{100}$	50 : 1	36%	10.4	15.2	1.46	271, 373	−41, 4
4	p(EVE)$_{100}$	100 : 1	44%	18.0	27.2	1.51	277, 379	−49, 4

[a] Standard reaction conditions: p(EVE) (4.0 μmol, 1 eq.), POPS (*n* eq.), TPPCl (0.33 eq.), DMAc (15 μM p(EVE)), 6 h, 60 °C. [b] Determined *via* ^{1}H NMR spectroscopy. [c] Determined *via* SEC in DMF with 0.025 M LiBr against PMMA standards. [d] Calculated from TGA thermograms. [e] Determined by DSC. p(EVE)$_{50}$: $M_n = 4.80$ kDa, $Đ = 1.27$. p(EVE)$_{100}$: $M_n = 7.17$ kDa, $Đ = 1.43$.

Table 3 Chain extensions of $p(EVE)_{50}$ with expanded thiirane scope[a]

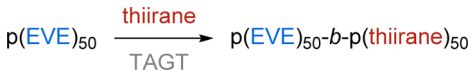

Entry	Thiirane	Conv.[b] (%)	M_n[c] (kDa)	$Đ$[c]	T_o[d] (°C)	T_g[e] (°C)
1[f]	PS	94	7.03	1.45	284, 403	−39, −31
2[f,g]	AOPS	45	6.90	1.35	284, 403	−53, −34
3[g,h]	PPS	>99	11.7	1.39	288, 399	−30, 7

[a] Standard reaction conditions: p(EVE) (4.0 μmol, 1 eq.), thiirane (50 eq.), TPPCl (0.33 eq.), DMAc (0.27 mL), 3 h, 60 °C. [b] Determined *via* ^{1}H NMR spectroscopy of the crude reaction mixture. [c] Determined *via* SEC in DMF with 0.025 M LiBr against PMMA standards. [d] Calculated from TGA thermograms. [e] Determined by DSC. [f] Starting from $p(EVE)_{50}$: M_n = 4.45 kDa, $Đ$ = 1.26. [g] 18 h reaction time. [h] Starting from $p(EVE)_{50}$: M_n = 4.23 kDa, $Đ$ = 1.29.

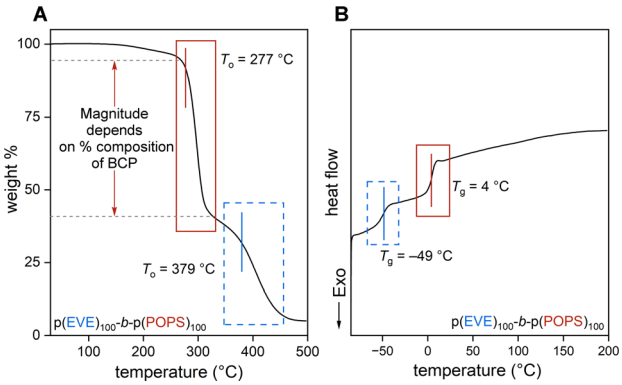

Fig. 5 (A) TGA and (B) DSC of $p(EVE)_{100}$-*b*-$p(POPS)_{100}$ with T_o and T_g features corresponding to p(POPS) (solid red box) and p(EVE) (dashed blue box) highlighted.

PPS in the homopolymerization studies (Fig. 3B) we increased the polymerization time for the chain extension experiments using these monomers. In 18 hours, AOPS only achieved 45% conversion (entry 2), whereas PPS reached full conversion (entry 3). In both cases, the resulting BCP maintained a narrow $Đ$ (1.35 and 1.39, respectively).

End-group analysis

In order to verify the presence of the trithiocarbonate end-group, we conducted COSY, HSQC, and HMBC NMR spectroscopy experiments (see Section S2.H†). To increase the relative intensity of the end-group peaks, low [monomer] : [**TCT3**] polymers ($p(EVE)_{10}$ and $p(EVE)_{10}$-*b*-$p(POPS)_{10}$) were synthesized. We utilized the 2D NMR spectra to assign the ^{1}H and ^{13}C peaks of each polymer.

The HMBC spectrum of $p(EVE)_{10}$ (Fig. S26†) showed correlations between the thiocarbonyl carbon and both the methylene of the thiyl end-group and the methine of the adjacent repeat unit. Additionally, MALDI-TOF MS analysis validated the desired end-groups for p(EVE) (Table S7 and Fig. S30 and S31†). For $p(EVE)_{10}$-*b*-$p(POPS)_{10}$ (Fig. S29†), a similar HMBC correlation between the thiocarbonyl carbon with the methylene of the adjacent repeat unit was observed. These experiments, along with the successful chain extensions, provide evidence that the trithiocarbonate chain end has been retained through both homopolymerization and diblock formation.

Thermal analysis

Next, we investigated the thermal properties of the BCPs purified by prepSEC. Extrapolated onset temperatures of degradation (T_os) were calculated from TGA thermograms and compared to the corresponding homopolymers (see Section S2.I†). All p(EVE)-*b*-p(POPS) BCPs had two major mass-loss features: T_o = 271–283 °C and 373–379 °C, corresponding to the p(POPS) and p(EVE) blocks, respectively (Fig. 5A and S39–S42†). As expected, the extent of each mass loss event corresponds to the size of the associated block. For example, the p(POPS) T_o accounts for approximately 33%, 50%, and 67% of the total mass loss for $p(EVE)_{100}$-*b*-$p(POPS)_{50}$ (Fig. S41†), $p(EVE)_{100}$-*b*-$p(POPS)_{100}$ (Fig. 5A), $p(EVE)_{50}$-*b*-$p(POPS)_{100}$ (Fig. S40†), respectively. A small mass-loss event is seen for each BCP around 150 °C which was also observed in the multi-stage degradation of the p(EVE) homopolymer (Fig. S32†).

Similarly, the PS-, AOPS-, and PPS-based BCPs displayed two major mass loss events with observed T_o values of 284–288 °C and 399–403 °C (Table 3 and Fig. S43–S45†). The intensities of these losses match well with the mass of each block.

DSC for each BCP revealed two T_g features (Fig. 5B, Tables 2 and 3, and Fig. S53–S59†), indicating that microphase separation between the two blocks has occurred.[63] The T_gs of the diblocks match closely to their respective homopolymers (Fig. S46, S47, S50–S52, Table S8†): the T_g at −49 to 30 °C originates from the p(EVE) block, and the other T_g originates from the thiirane block (p(POPS): 4–19 °C, p(PS): −39 °C, p(AOPS): −53 °C, p(PPS): 7 °C).

BCPs from three-mechanisms and three-monomer classes

Now that a **TCT** universal mediator can successfully combine cationic and anionic polymerizations, we wanted to demonstrate the power of this approach by expanding to three-mechanism BCPs. Because the **TCT** remains on the chain end, we were able to take advantage of its generality to change between photo-CP, TAGT, and now radical polymerization without intermediate steps. To accomplish this, the newly synthesized $p(EVE)_{50}$-*b*-$p(POPS)_{50}$ was chain extended using photocontrolled radical polymerization[46,71–80] of NIPAM (50 eq. relative to **TCT**) to make a novel terpolymer (Fig. 6).

Gratifyingly, we observed another significant shift of the SEC peak to a shorter retention time (Fig. 6), indicating successful triblock formation. Chain extension was also observed in another trial with block lengths of 100 for each block (see Section S2.J†). To the best of our knowledge, Kamigaito and coworkers reported[81] the only other example of sequentially combining anionic, cationic, and radical polymerizations, but their system did not use a different monomer class for each mechanism and required end-group modification after the anionic step. Therefore, our protocol represents the first report

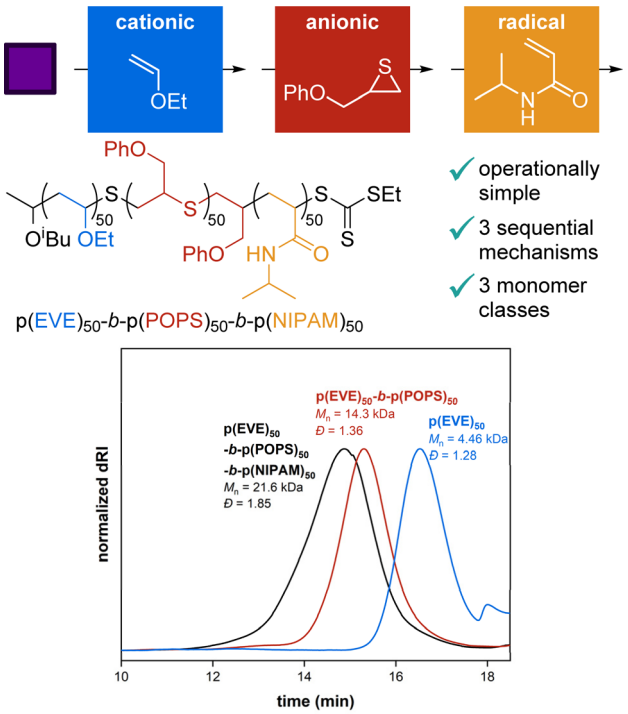

Fig. 6 SEC traces showing chain extension to a three-mechanism, three-monomer-class BCP. Radical polymerization conditions: p(EVE)-*b*-p(POPS) (4.0 μmol, 1 eq.), NIPAM (50 or 100 eq.), DCM (3 mM), $Ir(ppy)_3$ (0.045 mol% relative to NIPAM), RT, 456 nm LED, 6 h.

combining cationic, anionic, and radical polymerizations without any intermediate compatibilization or end-group modification steps to synthesize a BCP of three different monomer classes.

Conclusions

In summary, we identified and applied **TCT3** as a universal mediator for photo-CP and TAGT in a simple, sequential procedure. The proper selection of the R and Z groups of the **TCT** and determining the importance of p(EVE)'s solubility in DMAc enabled this approach. Clean shifts in the SEC traces support complete chain extension with a variety of thiiranes to form novel diblock copolymers. In particular, p(EVE)-*b*-p(POPS) BCPs were prepared with a range of block lengths. These materials exhibited two T_g features in the DSC thermograms, suggesting microphase separation into two distinct domains. The fidelity of the trithiocarbonate chain end was characterized by 2D NMR experiments and further demonstrated by a second chain extension using radical polymerization of NIPAM to form a three-monomer-class triblock terpolymer using three different mechanisms. Future work will focus on expanding the utility of this system as well as further characterization and application of these novel materials.

Data availability

The data supporting this article have been included as part of the ESI.†

Author contributions

The manuscript was written through contributions of all authors. All authors have given approval to the final version of the manuscript. Credit: **Brandon M. Hosford** data curation, formal analysis, investigation, methodology, validation, visualization, writing – original draft, and writing – review & editing; **William Ramos** data curation, formal analysis, investigation, methodology, visualization, writing – original draft, and writing – review & editing; **Jessica R. Lamb** conceptualization, formal analysis, funding acquisition, project administration, resources, supervision, writing – original draft, and writing – review & editing.

Conflicts of interest

There are no conflicts to declare.

Acknowledgements

This work was supported by the National Science Foundation (NSF) Materials Research Science and Engineering Center (MRSEC) (DMR-2011401) and the University of Minnesota (UMN). W. R. was partially supported by the 3M Science and Technology Graduate Fellowship. We thank Prof. Aleksandr Zhukhovitskiy and Hilary Djomnang-Fokwa for assistance with running prepSEC. NMR analyses were done in the Nuclear Magnetic Resonance Laboratory and the Minnesota NMR Center, which are supported by the Research and Innovation Office (RIO), the Medical School, the College of Biological Science, College of Science and Engineering (CSE), and the Department of Chemistry at UMN, and the Office of the Director, National Institutes of Health (NIH, S10OD011952), the NSF, and the Minnesota Medical Foundation. Mass spectrometry analysis was performed at the UMN Department of Chemistry Mass Spectrometry Laboratory (MSL), supported by RIO, CSE, and the Department of Chemistry at UMN, as well as the NSF (CHE-1336940). Part of this work was carried out in the CSE Polymer Characterization Facility at UMN, which has received capital equipment funding from the National Science Foundation through the UMN MRSEC. The content of this paper is the sole responsibility of the authors and does not represent the official views of or endorsement by the NIH or NSF.

Notes and references

1 H. J. Harwood, *Angew. Chem., Int. Ed. Engl.*, 1965, **4**, 1051–1060.
2 J.-F. Lutz, in *Sequence-Controlled Polymers: Synthesis, Self-Assembly, and Properties*, American Chemical Society, 2014, vol. 1170, pp. 1–11.
3 J. G. Baker, R. Zhang and C. A. Figg, *J. Am. Chem. Soc.*, 2024, **146**, 106–111.
4 R. B. Grubbs and R. H. Grubbs, *Macromolecules*, 2017, **50**, 6979–6997.
5 G. K. K. Clothier, T. R. Guimarães, S. W. Thompson, J. Y. Rho, S. Perrier, G. Moad and P. B. Zetterlund, *Chem. Soc. Rev.*, 2023, **52**, 3438–3469.

6 D. J. Keddie, *Chem. Soc. Rev.*, 2013, **43**, 496–505.
7 K. Min, H. Gao and K. Matyjaszewski, *J. Am. Chem. Soc.*, 2005, **127**, 3825–3830.
8 K. Matyjaszewski and J. Spanswick, *Mater. Today*, 2005, **8**, 26–33.
9 Y. K. Chong, T. P. T. Le, G. Moad, E. Rizzardo and S. H. Thang, *Macromolecules*, 1999, **32**, 2071–2074.
10 G. Gody, T. Maschmeyer, P. B. Zetterlund and S. Perrier, *Nat. Commun.*, 2013, **4**, 2505.
11 M. Ouchi and M. Sawamoto, *Polym. J.*, 2018, **50**, 83–94.
12 N. Ekizoglou and N. Hadjichristidis, *J. Polym. Sci., Part A: Polym. Chem.*, 2002, **40**, 2166–2170.
13 T. P. Lodge and P. C. Hiemenz, in *Polymer Chemistry*, CRC Press, Taylor and Francis Group, Boca Raton, 3rd edn, 2020.
14 A. Favier and M.-T. Charreyre, *Macromol. Rapid Commun.*, 2006, **27**, 653–692.
15 G. Moad, J. Chiefari, Y. K. Chong, J. Krstina, R. T. Mayadunne, A. Postma, E. Rizzardo and S. H. Thang, *Polym. Int.*, 2000, **49**, 993–1001.
16 M. Khan, T. R. Guimarães, K. Choong, G. Moad, S. Perrier and P. B. Zetterlund, *Macromolecules*, 2021, **54**, 736–746.
17 A. Dey, U. Haldar and P. De, *Front. Chem.*, 2021, **9**, 644547.
18 X.-H. Guo, G.-G. Gu, T.-J. Yue and W.-M. Ren, *Polym. Chem.*, 2023, **14**, 5034–5039.
19 S. Creutz, C. Vandooren, R. Jérôme and P. Teyssié, *Polym. Bull.*, 1994, **33**, 21–28.
20 A. Verma, A. Nielsen, J. E. McGrath and J. S. Riffle, *Polym. Bull.*, 1990, **23**, 563–570.
21 A. Puglisi, E. Murtezi, G. Yilmaz and Y. Yagci, *Polym. Chem.*, 2017, **8**, 7307–7310.
22 M. U. Kahveci, G. Acik and Y. Yagci, *Macromol. Rapid Commun.*, 2012, **33**, 309–313.
23 S. Kumagai, K. Nagai, K. Satoh and M. Kamigaito, *Macromolecules*, 2010, **43**, 7523–7531.
24 M. Schäfer, P. C. Wieland and O. Nuyken, *J. Polym. Sci., Part A: Polym. Chem.*, 2002, **40**, 3725–3733.
25 J. Feldthusen, B. Iván and A. H. E. Müller, *Macromolecules*, 1997, **30**, 6989–6993.
26 E. Yoshida and A. Sugita, *Macromolecules*, 1996, **29**, 6422–6426.
27 R. Nomura, M. Narita and T. Endo, *Macromolecules*, 1994, **27**, 4853–4854.
28 Q. Liu, M. Konas, R. M. Davis and J. S. Riffle, *J. Polym. Sci., Part A: Polym. Chem.*, 1993, **31**, 1709–1717.
29 S. Nemes and J. P. Kennedy, *J. Macromol. Sci., Chem.*, 1991, **28**, 311–328.
30 T. Kitayama, T. Nishiura and K. Hatada, *Polym. Bull.*, 1991, **26**, 513–520.
31 T. Souel, F. Schué, M. Abadie and D. H. Richards, *Polymer*, 1977, **18**, 1292–1294.
32 F. J. Burgess, A. V. Cunliffe, J. R. MacCallum and D. H. Richards, *Polymer*, 1977, **18**, 726–732.
33 F. J. Burgess, A. V. Cunliffe, J. R. MacCallum and D. H. Richards, *Polymer*, 1977, **18**, 719–725.
34 F. J. Burgess, A. V. Cunliffe, J. V. Dawkins and D. H. Richards, *Polymer*, 1977, **18**, 733–740.
35 K. Zhang, T. Bai and J. Ling, *Macromolecules*, 2023, **56**, 7389–7395.
36 H. Qiu, T. Shen, Z. Yang, F. Wu, X. Li, Y. Tu and J. Ling, *Chin. J. Chem.*, 2022, **40**, 705–712.
37 H. Dong, Y. Zhu, Z. Li, J. Xu, J. Liu, S. Xu, H. Wang, Y. Gao and K. Guo, *Macromolecules*, 2017, **50**, 9295–9306.
38 Y. Hepuzer, Y. Yagci, T. Biedron and P. Kubisa, *Angew. Makromol. Chem.*, 1996, **237**, 163–171.
39 M. Guerre, M. Uchiyama, E. Folgado, M. Semsarilar, B. Améduri, K. Satoh, M. Kamigaito and V. Ladmiral, *ACS Macro Lett.*, 2017, **6**, 393–398.
40 M. Uchiyama, K. Satoh and M. Kamigaito, *Angew. Chem., Int. Ed.*, 2015, **54**, 1924–1928.
41 Q. Ma, X. Zhang, Y. Jiang, J. Lin, B. Graff, S. Hu, J. Lalevée and S. Liao, *Polym. Chem.*, 2022, **13**, 209–219.
42 V. Kottisch, Q. Michaudel and B. P. Fors, *J. Am. Chem. Soc.*, 2017, **139**, 10665–10668.
43 Y. Ma, V. Kottisch, E. A. McLoughlin, Z. W. Rouse, M. J. Supej, S. P. Baker and B. P. Fors, *J. Am. Chem. Soc.*, 2021, **143**, 21200–21205.
44 M. J. Supej, B. M. Peterson and B. P. Fors, *Chem*, 2020, **6**, 1794–1803.
45 A. Nagai, N. Koike, H. Kudo and T. Nishikubo, *Macromolecules*, 2007, **40**, 8129–8131.
46 Z. Zhang, T.-Y. Zeng, L. Xia, C.-Y. Hong, D.-C. Wu and Y.-Z. You, *Nat. Commun.*, 2018, **9**, 2577.
47 J.-W. Li, M. Chen, Z. Zhang, C.-Y. Pan, W.-J. Zhang and C.-Y. Hong, *Polym. Chem.*, 2022, **13**, 402–410.
48 Z. Zhang, L. Xia, T.-Y. Zeng, D.-C. Wu, W.-J. Zhang, C.-Y. Hong and Y.-Z. You, *Polym. Chem.*, 2019, **10**, 2117–2125.
49 C.-H. Wang, Y.-S. Fan, Z. Zhang, Q.-B. Chen, T.-Y. Zeng, Q.-Y. Meng and Y.-Z. You, *Appl. Surf. Sci.*, 2019, **475**, 639–644.
50 M. K. Gupta, T. A. Meyer, C. E. Nelson and C. L. Duvall, *J. Controlled Release*, 2012, **162**, 591–598.
51 S. W. Spring, C. S. Cerione, J. H. Hsu, S. L. Shankel and B. P. Fors, *Chin. J. Chem.*, 2023, **41**, 399–404.
52 S. L. Shankel, T. H. Lambert and B. P. Fors, *Polym. Chem.*, 2022, **13**, 5974–5979.
53 B. M. Peterson, S. Lin and B. P. Fors, *J. Am. Chem. Soc.*, 2018, **140**, 2076–2079.
54 J. Li, A. Kerr, Q. Song, J. Yang, S. Häkkinen, X. Pan, Z. Zhang, J. Zhu and S. Perrier, *ACS Macro Lett.*, 2021, **10**, 570–575.
55 M. Matsuda, M. Uchiyama, Y. Itabashi, K. Ohkubo and M. Kamigaito, *Polym. Chem.*, 2022, **13**, 1031–1039.
56 X. Zhang, Y. Jiang, Q. Ma, S. Hu and S. Liao, *J. Am. Chem. Soc.*, 2021, **143**, 6357–6362.
57 S. Singha, S. Pan, S. S. Tallury, G. Nguyen, R. Tripathy and P. De, *ACS Polym. Au*, 2024, **3**, 189–207.
58 P. C. Knutson, A. J. Teator, T. P. Varner, C. T. Kozuszek, P. E. Jacky and F. A. Leibfarth, *J. Am. Chem. Soc.*, 2021, **143**, 16388–16393.
59 Z. Zhang, X. Nie, F. Wang, G. Chen, W.-Q. Huang, L. Xia, W.-J. Zhang, Z.-Y. Hao, C.-Y. Hong, L.-H. Wang and Y.-Z. You, *Nat. Commun.*, 2020, **11**, 3654.
60 A. Takahashi, S. Tsunoda, R. Yuzaki and A. Kameyama, *Macromolecules*, 2020, **53**, 5227–5236.

61 M. R. Hill, R. N. Carmean and B. S. Sumerlin, *Macromolecules*, 2015, **48**, 5459–5469.
62 M.-N. Antonopoulou, R. Whitfield, N. P. Truong and A. Anastasaki, *Eur. Polym. J.*, 2022, **174**, 111326.
63 H. Daimon, H. Okitsu and J. Kumanotani, *Polym. J.*, 1975, **7**, 460–466.
64 V. Kottisch, Q. Michaudel and B. P. Fors, *J. Am. Chem. Soc.*, 2016, **138**, 15535–15538.
65 B. M. Peterson, V. Kottisch, M. J. Supej and B. P. Fors, *ACS Cent. Sci.*, 2018, **4**, 1228–1234.
66 Q. Michaudel, T. Chauviré, V. Kottisch, M. J. Supej, K. J. Stawiasz, L. Shen, W. R. Zipfel, H. D. Abruña, J. H. Freed and B. P. Fors, *J. Am. Chem. Soc.*, 2017, **139**, 15530–15538.
67 A high degree of purity is needed to polymerize EVE with **TCT1**.[66]
68 V. Kottisch, M. J. Supej and B. P. Fors, *Angew. Chem., Int. Ed.*, 2018, **57**, 8260–8264.
69 S. W. Spring, J. H. Hsu, R. J. Sifri, S.-M. Yang, C. S. Cerione, T. H. Lambert, C. J. Ellison and B. P. Fors, *J. Am. Chem. Soc.*, 2022, **144**, 15727–15734.
70 H. Cramail and A. Deffieux, *Macromol. Chem. Phys.*, 1994, **195**, 217–227.
71 J. Xu, C. Fu, S. Shanmugam, C. J. Hawker, G. Moad and C. Boyer, *Angew. Chem., Int. Ed.*, 2017, **56**, 8376–8383.
72 M. Chen, S. Deng, Y. Gu, J. Lin, M. J. MacLeod and J. A. Johnson, *J. Am. Chem. Soc.*, 2017, **139**, 2257–2266.
73 J. Xu, S. Shanmugam, C. Fu, K.-F. Aguey-Zinsou and C. Boyer, *J. Am. Chem. Soc.*, 2016, **138**, 3094–3106.
74 S. Shanmugam, J. Xu and C. Boyer, *Angew. Chem., Int. Ed.*, 2016, **55**, 1036–1040.
75 J. Xu, S. Shanmugam, H. T. Duong and C. Boyer, *Polym. Chem.*, 2015, **6**, 5615–5624.
76 S. Shanmugam, J. Xu and C. Boyer, *Chem. Sci.*, 2015, **6**, 1341–1349.
77 S. Shanmugam, J. Xu and C. Boyer, *J. Am. Chem. Soc.*, 2015, **137**, 9174–9185.
78 S. Shanmugam and C. Boyer, *J. Am. Chem. Soc.*, 2015, **137**, 9988–9999.
79 M. Chen, M. J. MacLeod and J. A. Johnson, *ACS Macro Lett.*, 2015, **4**, 566–569.
80 J. Xu, K. Jung, A. Atme, S. Shanmugam and C. Boyer, *J. Am. Chem. Soc.*, 2014, **136**, 5508–5519.
81 K. Satoh, Y. Mori and M. Kamigaito, *J. Polym. Sci., Part A: Polym. Chem.*, 2019, **57**, 465–473.